Evaluating Southern Ocean Response to Wind Forcing

Sarah T. Gille*

School of Environmental Sciences, University of East Anglia, UK

Camera-ready Copy for

Physics and Chemistry of the Earth

Manuscript-No. G5-032

Offset requests to:
Sarah T. Gille
Department of Earth System Science, University of California, Irvine, CA 92697-3100, USA

*Present address Department of Earth System Science, University of California, Irvine, CA 92697-3100 USA

Evaluating Southern Ocean Response to Wind Forcing

Sarah T. Gille*

School of Environmental Sciences, University of East Anglia, UK

*Present address Department of Earth System Science, University of California, Irvine, CA 92697-3100 USA

1 Resume

In order to investigate how the Antarctic Circumpolar Current (ACC) responds to changes in wind forcing, cross coherences are calculated between Southern Ocean winds and bottom pressure measurements from either side of Drake Passage. Wind stress and wind-stress curl are derived from the European Research Satellites (ERS) scatterometers, from the Special Sensor Microwave Imager (SSMI), and from the European Centre for Medium-Range Weather Forecasts (ECMWF) forecast model. Winds and bottom pressure measurements both show substantial variability on all resolved time scales. Statistically significant coherences occur over the full range of resolved frequencies for both wind stress and wind-stress curl. The largest number of statistically coherent frequencies occur between the bottom pressure at the south side of Drake Passage and wind stress. Phases are consistent with wind slightly leading bottom pressure, and strong winds driving strong transport.

2 Introduction

Winds over the Southern Ocean are among the strongest in the world, but the magnitude and variability of these winds is not well known. Because of the paucity of in situ measurements, Southern Ocean wind fields derived from numerical models have been suspect.

In this study new satellite wind measurements provide a more accurate means to estimate changes in wind forcing of the Antarctic Circumpolar Current (ACC). Wind measurements are compared with bottom pressure measurements from Drake Passage. This information is used to address two questions. First, how does the ocean respond to changes in wind? And second, is there a detectable difference between the ocean's response to wind stress and wind-stress curl?

The question of how the Southern Ocean responds to wind forcing has been a subject of vociferous debate since the early 1950s. One view of the ACC proposes that wind stress input at the surface is removed through bottom form stress (Munk and Palmén, 1951). In this scheme, momentum is carried down through the water column via interfacial form stress. Based on this idea, Johnson and Bryden (1989) suggested the relation:

$$T \propto \sqrt{\tau^x} \quad (1)$$

where τ^x is the zonal wind stress, and T is transport.

As an alternative to the direct forcing mechanism, Stommel (1957) pointed out that wind-stress curl might drive the ACC, in analogy with mid-latitude Sverdrup dynamics. Based on heat budget considerations, Warren et al. (1996) argued in favor of balance of the form:

$$T \propto \mathrm{curl}\, \tau. \quad (2)$$

In response to this debate, Gnanadesikan and Hallberg (1998) used numerical model output to consider the relative importance of wind stress, wind-stress curl, and thermodynamics in controlling Circumpolar Current transport. Their model circulations displayed some characteristics of wind-stress forcing and some characteristics of Sverdup balance, although they concluded that buoyancy forcing plays an essential role in determining mean zonal transport in their test cases. In this framework, wind-driven surface Ekman flux can fix the mixed-layer depth and therefore contribute directly to the buoyancy forcing.

While these considerations focused on the the processes controlling mean ACC transport, fluctuations in transport are likely to respond to fluctuations in wind in an analogous way. This study uses direct observations of the Southern Ocean to consider whether the system responds more strongly to wind stress or wind-stress curl. Section 2 describes the data used in this analysis. Section 3 outlines the basic results of the coherence analysis. The results are summarized and discussed in Section 4.

3 Measurements

3.1 Wind

The scatterometers aboard the European Research Satellites (ERS-1 and ERS-2) have measured wind over the global ocean since August 1991. Scatterometers measure radar backscatter off capillary waves, which allows them to determine both wind speed and direction, although the backscatter solution allows the possibility of four possible wind directions, and the most typical errors are wrong by 180°. Two separate ERS wind products are considered in this study.

First, weekly fields of ERS scatterometer wind stress and wind-stress curl were provided by the French Centre ERS d'Archivage et de Traitement (CERSAT). CERSAT maps wind vectors using a minimum variance method which is related to Kriging (Bentamy et al., 1996).

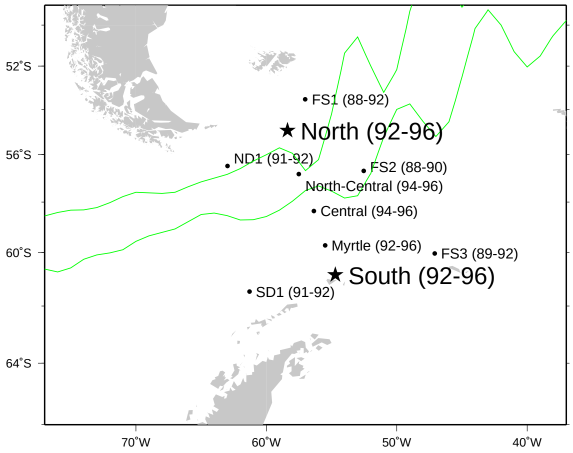

Fig. 1. Locations of bottom pressure gauges deployed by Proudman Oceanographic Laboratory in Drake Passage since 1988. The north and south stations, marked with stars, are the focus of this study. The gray lines indicate the estimated mean locations of the Subantarctic and Polar Fronts of the ACC.

In addition, raw wind vectors from ERS-1 and ERS-2 are also used. This study considers the data set released by the U.S. Jet Propulsion Laboratory (JPL) based on the work of Freilich and Dunbar (1993). For the present study, winds were bin-averaged at daily intervals, and then either zonally averaged with a 1° longitude window or box averaged in a 2° latitude by 2° longitude box around the bottom pressure recorder sites. Binning raw data can leave substantial data gaps, but it avoids interpolating where no data exist.

Two other wind fields have also been examined. The Special Sensor Microwave Imager (SSMI) satellite instrument measures wind speed but not direction. JPL determines wind vectors using a 2D variational analysis method to combine information from European Centre for Medium-Range Weather Forecasts (ECMWF) 10 m winds and ship and buoy winds with the SSMI wind speed estimates. This study uses JPL's gridded winds at 2° latitude by 2.5° longitude by 5-day resolution.

Finally, from the ECMWF analysis, numerical forecast winds at 12-hour intervals are available in the time period from 1992 to 1995.

3.2 Bottom Pressure

Since 1988, Proudman Oceanographic Laboratory has deployed bottom pressure gauges in Drake Passage as part of the extensive ACCLAIM bottom pressure monitoring program (Antarctic Circumpolar Current Levels by Altimetry and Island Measurements) shown in Fig. 1. Gauges were ordinarily deployed and recovered in November of each year, though the 1994 deployment stayed in for two years. The focus of this study will be the four-year time series from 1992 through 1996 at the north and south BPRs, marked with stars in Fig. 1.

From Topex altimeter measurements, the mean path of the ACC has been estimated using the method described by Gille (1994). This indicates that the northern-

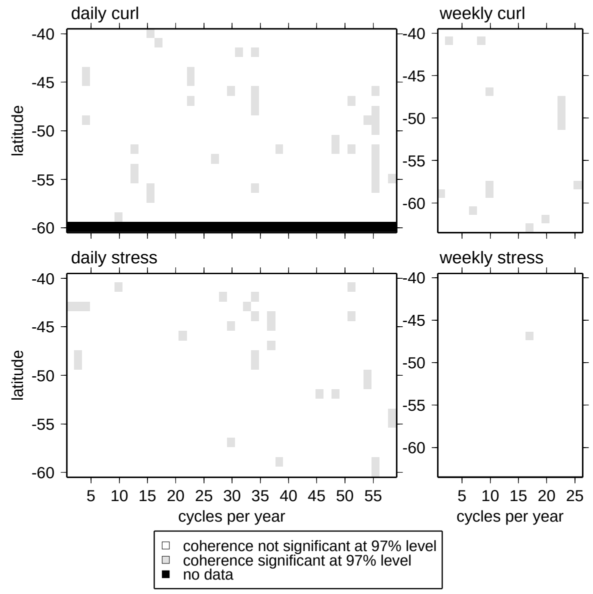

Fig. 2. Coherence of north BPR and zonally-averaged scatterometer wind stress curl (upper panels) and wind stress (lower panels). Daily winds (left) refer to bin-averaged raw scatterometer wind vectors from JPL (see text). Weekly winds (right) are from the gridded wind product produced by CERSAT.

most BPRs are north of the Subantarctic Front of the ACC, though they are close enough to it that they may feel the effects of the meandering current. The southern BPR is well south of the Polar Front.

Using the geostrophic relationship, we can estimate barotropic transport of the ACC by calculating the difference between bottom pressure on the northern and southern sides of the ACC. However the data are noisy, and the difference is even noisier. Hughes et al. (1998) have suggested that bottom pressure at the north may be contaminated by the effects of the subtropical gyre, so that southern bottom pressure will be a better proxy for transport fluctuations. In this analysis the north BPR, the south BPR, and the differences between them are all used.

4 Coherence between Wind and Transport

Since Drake Passage is a choke point for the ACC, past studies have conjectured that the transport through Drake Passage should respond to changes in the global wind forcing (e.g., Peterson, 1988; Wearn and Baker, 1980). Thus this study will look at zonally-averaged winds between 40°S and 63°S as well as local winds near the BPRs.

Coherence analysis techniques are used to identify the frequencies at which the ocean most closely resembles the wind. Data are broken into 256-day segments, overlapping by 128 days. A Hanning window is applied to the data, and Fast Fourier Transforms are computed. These are averaged to estimate coherences.

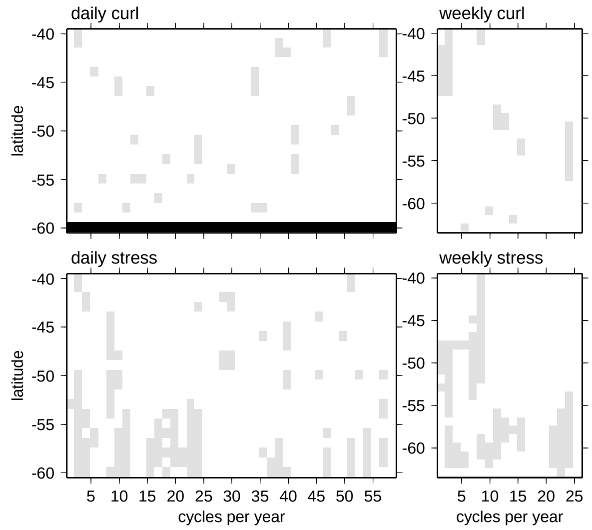

Fig. 3. Coherence of south BPR and zonally-averaged scatterometer winds as in Fig. 2.

Because there are missing data, error analysis is carried out using Monte Carlo techniques. Coherences of white noise containing the same gaps as the original data are computed, and from these 97% confidence limits are estimated.

Figure 2 shows the frequencies and latitudes of zonally-averaged daily and weekly scatterometer wind that are coherent at the "97%" significance level with the north BPR. Upper panels show coherence between bottom pressure and wind-stress curl, indicative of the Sverdrup-type dynamics advocated by Warren et al. (1996). Lower panels show the coherence of bottom pressure to wind stress, corresponding to the form stress balancing wind stress model of the ACC. (Results for the model-based winds from ECMWF and SSMI winds are not depicted here.)

Significant coherences for the daily winds are shown between 1 and 41 cycles per 256 days. Higher frequencies are not shown because data drop out and noise make the results more suspect. Since the CERSAT weekly winds have a lower Nyquist frequency, significant coherences are indicated in the range from 1 to 18 cycles per 256 days. Wind and bottom pressure are statistically coherent at few frequency-latitude combinations. In general, the north BPR is more often coherent with wind-stress curl than with wind-stress, and it is more coherent with wind-stress at latitudes north of Drake Passage.

In contrast, bottom pressure on the south side of Drake Passage shows very different patterns of coherence, as depicted in Fig. 3. The south BPR is more often coherent with wind stress than with wind-stress curl, and it responds more strongly to winds within the latitude of Drake Passage. These findings are consistent with the results of Hughes et al. (1998).

In Fig. 4 the pressure difference between the north and south BPR locations is noisier and less statistically coherent with wind than the south BPR. Coherence patterns resemble those seen at the south BPR.

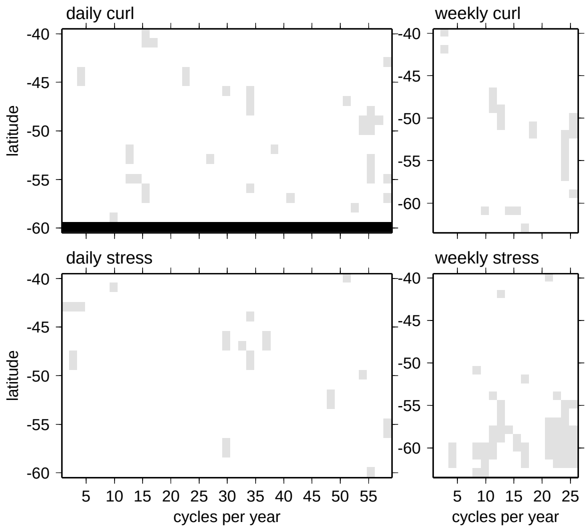

Fig. 4. Coherence of north minus south BPR and zonally-averaged scatterometer winds as in Fig. 2.

To test whether these results are different from the null hypothesis that wind and BPR time series are uncorrelated white noise processes, we count the number of significantly coherent points compared with the total number of points in each figure. For pure white noise, roughly 3.8% of points should exceed the "97%" confidence limit determined in this Monte Carlo analysis. In Table 1 coherence ratios that exceed the white noise prediction by one standard deviation are marked in bold type. Table 1 indicates that for the wind products considered here, the north BPR is usually coherent at more frequencies and latitudes with wind-stress curl than with wind stress, the south BPR is always coherent at more frequency-latitude combinations with wind stress, and the bottom-pressure difference is similar to the south BPR.

Overall this analysis of zonally-averaged winds suggests that the Sverdrup balance between wind-stress curl and ocean transport is more likely to be important at latitudes on the north side and north of Drake Passage, where continental boundaries may help to set up gyre circulation. In the latitudes of Drake Passage (and particularly on the south side of the Passage), where no meridional boundaries control the flow, bottom pressure appears to vary in direct response to wind stress.

In addition to responding to variations in zonally-averaged winds, the transport through Drake Passage may also be influenced by local winds. For this study, local winds are determined by averaging wind values from grid points near the North, North-Central, Central, Myrtle, and South BPRs shown in Figure 1. Since the resolution of the wind fields varies, winds are averaged over 1° by 1° for weekly CERSAT winds, 2° by 2° for daily scatterometer winds, 2° by 2.5° SSMI winds, and 3° by 3° for ECMWF. Time series of local winds have more gaps, making the significance criteria much stricter. As shown in Table 1, in most cases bottom pressure is less likely to be coherent with local winds than with zonally-averaged winds. For the daily scatterometer and 12-hour ECMWF winds, local wind stress rather than

zonally-averaged winds					
		daily	weekly	SSMI	ECMWF
North BPR	curl	**4.6%**	3.2%	4.4%	2.9%
	stress	3.4%	0.2%	4.6%	2.7%
South BPR	curl	**4.8%**	**7.6%**	2.2%	**6.8%**
	stress	**15.5%**	**20.8%**	**7.1%**	**12.7%**
N-S BPR	curl	4.4%	**5.6%**	1.7%	**9.0%**
	stress	2.7%	**13.0%**	3.0%	**12.4%**
local winds					
		daily	weekly	SSMI	ECMWF
North BPR	curl	1.6%	**7.8%**	1.7%	**6.8%**
	stress	**5.4%**	1.1%	4.2%	**7.8%**
South BPR	curl	4.9%	5.6%	2.5%	**5.9%**
	stress	**16.6%**	4.4%	1.7%	**11.7%**
N-S BPR	curl	1.6%	4.4%	**5.8%**	**7.8%**
	stress	3.9%	**6.7%**	0.8%	**15.1%**

Table 1. Percentage of frequency–latitude points at which wind is statistically coherent with the north BPR, the south BPR, or the difference between the two. For white noise, this percentage is predicted to be 3.8%. Wind fields for which these percentages are at least one standard deviation greater than 3.8% are bold.

local curl is more coherent with bottom pressure. No clear pattern emerges from the weekly CERSAT and 5-day SSMI winds.

Besides showing the simple coherence as a function of frequency, coherence analysis also determines the phase relationship between wind and bottom pressure. Phase estimates are meaningful only at frequencies for which the measurements are statistically coherent. Figures 5, 6, and 7 show histograms of phases for statistically significant frequency-latitude pairs for the north BPR, the south BPR, and the north–south pressure difference, respectively. In addition, phases of individual statistically coherent points are plotted against frequency in the radial direction, with low frequencies near the origin and high frequencies on the outside.

The phases of coherent frequencies for the northern BPR in Fig. 5 are scattered almost equally between 0° and 360°. For the southern BPR in Fig. 6, wind-stress curl has no dominant phase relationship with transport, while the phase difference between wind stress and southern bottom pressure is predominantly between 150° and 180°. As the distribution of small letters in Fig. 6 indicates, this is true almost regardless of frequency. Similarly, the north–south pressure difference in Fig. 7 shows no dominant phase relationship with wind-stress curl, but tends to have phases between 300° and 0° relative to wind stress at low frequency.

Phase differences near 180° for the southern BPR and near 0° for the north–south pressure difference indicate that strong winds are associated with strong pressure differences. In other words, strong eastward winds are associated with high eastward transport. The observed phase lags are slightly negative relative to the predicted phases, suggesting that wind slightly leads bottom pressure. Thus wind tends to accelerate the ocean.

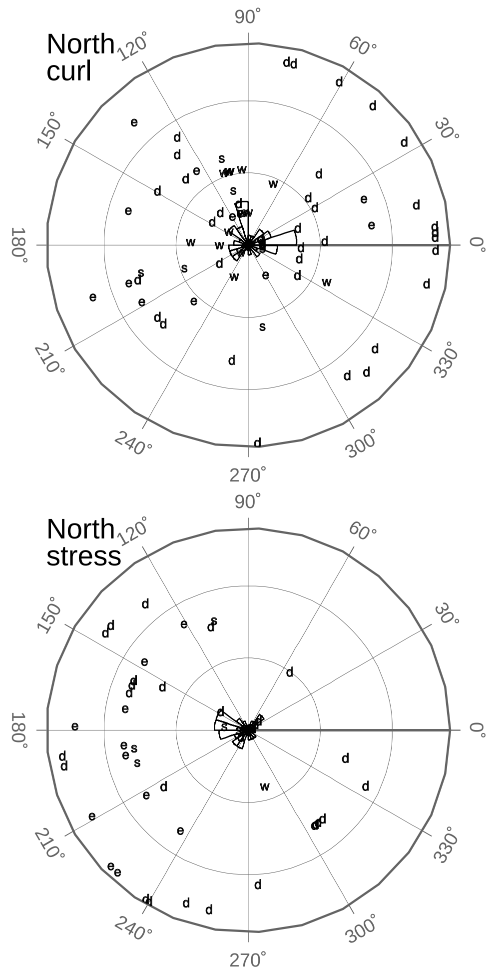

Fig. 5. Histograms of statistically significant phases (solid lines) for the north BPR compared with all four wind products combined. Grid circles indicate 15 and 30 points respectively. Letters show individual statistically coherent points phase–frequency space, with frequency indicated in radial distance, with grid lines at 15 and 30 cycles per 256 days. The highest frequency plotted is 41 cycles per 256 days. Letters correspond to the wind fields (d) daily from JPL, (w) weekly from CERSAT, (s) SSMI, and (e) ECMWF.

5 Summary

This study has computed coherences between bottom pressure in Drake Passage and four different wind fields in order to examine how the ACC responds to variations in wind.

No specific effort has been made in this study to determine the best wind product. If a desired characteristic of a wind field is that it be coherent with ocean transport over a broad range of frequencies and wind latitudes, then the bin-averaged daily scatterometer winds, CERSAT weekly scatterometer winds, and ECMWF analysis fields all have some advantages. The zonally-averaged CERSAT winds compare well with Drake Passage bottom pressures. For local analysis, more coherence is obtained from the more frequent daily scatterometer and ECMWF products.

Regardless of the wind product considered, results of this analysis indicate that the southern side of Drake Passage is more frequently coherent with wind stress than with wind-stress curl, while the north side is more frequently coherent with wind-stress curl. The north–south pressure difference is slightly more frequently coherent with stress than with curl.

Phase information is inconclusive for the north BPR and for wind-stress curl. At the south BPR, bottom pressure lags wind stress slightly, consistent with strong winds driving large transports.

Since bottom pressure measurements can be coherent with both wind-stress curl and with wind stress, both a Sverdrupian vorticity balance and direct wind forcing may influence the behavior of the ACC. However, the stronger coherence and more consistent phases due to wind stress suggest that for the time scales resolved in this study, the system behaves predominantly as if it is directly forced by the wind.

Acknowledgements. Comments from the reviewers and discussions with Kate Grose, Karen Heywood, Chris Hughes, Stefan Llewellyn Smith, Mike Meredith, and Dave Stevens have helped shape this study and its presentation. Proudman Oceanographic Laboratory has kindly made their bottom pressure measurements available. Measured wind data were provided by the US Jet Propulsion Laboratory and by CERSAT, which is part of IFREMER in Brest, France. This research was supported by a fellowship from the North Atlantic Treaty Organization awarded in 1997.

References

Bentamy, A., Grima, N., Quilfen, Y., Harscoat, V., Maroni, C., and Pouliquen, S., An atlas of surface wind from ers-1 scatterometer measurements, IFREMER publication, IFREMER, BP 70, 29280 Plouzané, France, 229 pp., 1996.

Freilich, M. H. and Dunbar, R. S., A preliminary C-band scatterometer model function for the ERS-1 AMI instrument, in *Proceedings First ERS-1 Symposium—Space at the Service of Our Environment, Cannes, France*, pp. 79–84, Eur. Space Agency Spec. Publ., ESA SP-359, 1993.

Gille, S. T., Mean sea surface height of the Antarctic Circumpolar Current from Geosat data: Method and application, *J. Geophys. Res.*, *99*, 18,255–18,273, 1994.

Gnanadesikan, A. and Hallberg, R. W., On the relationship of the Circumpolar Current to Southern Hemisphere winds, *J. Phys. Oceanogr.*, submitted, 1998.

Hughes, C. W., Meredith, M. P., and Heywood, K. J., Wind driven transport fluctuations through Drake Passage: a southern mode, *J. Phys. Oceangr.*, in press, 1998.

Johnson, G. C. and Bryden, H. L., On the size of the Antarctic Circumpolar Current, *Deep Sea Res.*, *36*, 39–53, 1989.

Munk, W. H. and Palmén, E., Note on the dynamics of the Antarctic Circumpolar Current, *Tellus*, *3*, 53–55, 1951.

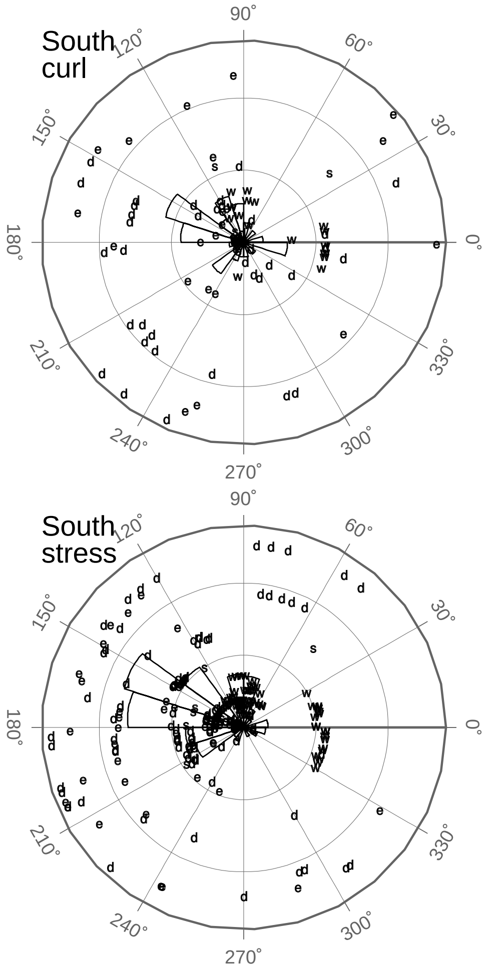

Fig. 6. Histograms and phase–frequency points for the south BPR, as in Fig. 5. Because of the large number of coherent points for wind stress, values in the stress histogram are scaled down by a factor of 2.

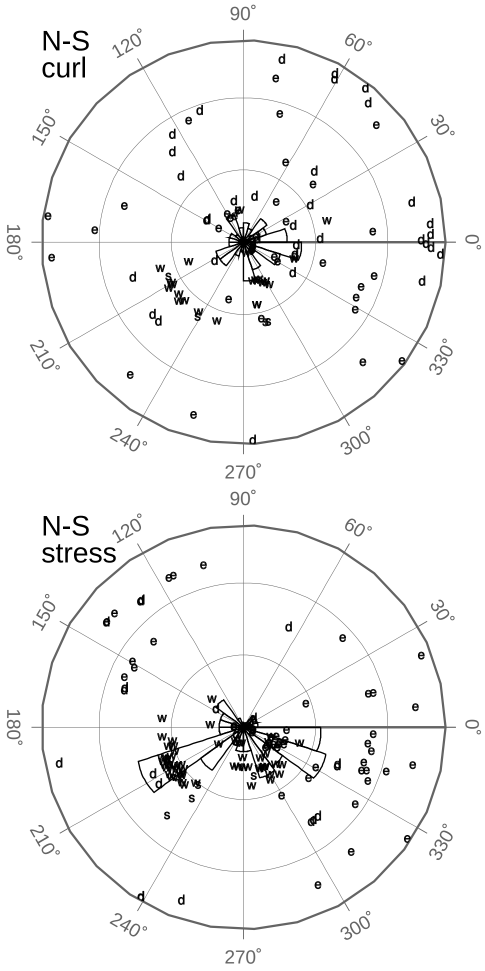

Fig. 7. Histograms and phase–frequency points for the north–south pressure difference, as in Fig. 5.

Peterson, R. G., On the transport of the Antarctic Circumpolar Current through Drake Passage and its relation to wind, *J. Geophys. Res.*, *93*, 13,993–14,004, 1988.

Stommel, H., A survey of ocean current theory, *Deep Sea Res.*, *4*, 149–184, 1957.

Warren, B. A., LaCasce, J. H., and Robbins, P. E., On the obscurantist physics of "Form drag" in theorizing about the Circumpolar Current, *J. Phys. Oceanogr.*, *26*, 2297–2301, 1996.

Wearn, Jr., R. B. and Baker, Jr., D. J., Bottom pressure measurements across the Antarctic Circumpolar Current and their relation to the wind, *Deep Sea Res.*, *27A*, 875–888, 1980.